# Linear Fresnel collector mirrors – Measured systematic surface errors and their impact on the focal line

Cite as: AIP Conference Proceedings **2126**, 100003 (2019); https://doi.org/10.1063/1.5117612
Published Online: 26 July 2019

Anna Heimsath, Peter Schöttl, Gregor Bern, and Peter Nitz



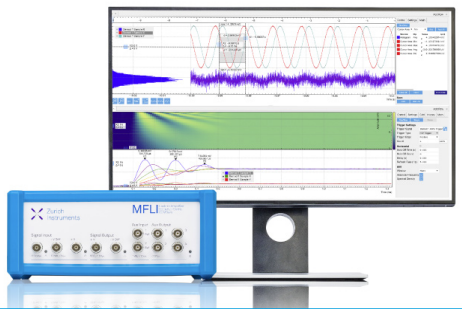

# Linear Fresnel Collector Mirrors – Measured Systematic Surface Errors and Their Impact on the Focal Line

Anna Heimsath[1, a)], Peter Schöttl[1], Gregor Bern[1] and Peter Nitz[1]

[1]*Fraunhofer Institute for Solar Energy Systems. Heidenhofstr. 2, 79110 Freiburg, Germany*

[a)]Corresponding author: anna.heimsath@ise.fraunhofer.de

**Abstract.** Objective of this article is to show and discuss the shape accuracy of solar reflector panels for linear Fresnel collectors. Systematic shape deviations due to torsion or orientation errors are responsible for severe optical losses and underperformance. This is why this article investigates systematic surface deviations beyond the standard quality parameters like SDx and FDy. We discuss typical characteristics of linear Fresnel collector reflector panels. Our measurement results show local surface slope deviations measured by deflectometry. In the second part of this study, the effect of systematic surface slope deviations is analyzed by use of a parametric model. We apply the model to detect systematic production errors, investigate optical losses and the impact on the focal line with ray tracing.

## INTRODUCTION

The linear Fresnel collector (LFC) follows the approach of Fresnel lenses, implying the approximation of the ideal curved shape of a large parabola by numerous almost flat reflector panels. The individual solar reflector panels of a LFC are usually symmetric sections of a parabolic cylinder with a width between 0.5m and 1m and several meters length, flat in the long, longitudinal dimension and slightly curved along the short, transversal dimension to focus the solar radiation. Small linear Fresnel collectors for process heat generation typically have reflector panels with focal lengths in the range of 4m-6m. Large LFC for solar power plants or other high temperature applications typically consist of reflector panels with focal lengths in the range of 8m-12m.

Due to the small curvature of reflector panels in LFCs it is possible to produce the curved surface by a variety of production processes, each of them exhibiting advantages and drawbacks with regard to accuracy, weight and cost. One of the first production processes developed for LFC mirrors envisioned low cost flat reflectors. Mirrors are bent elastically to procure the shape. The mirrors are assembled on curved jigs; the glass is fixed by adhesive onto a frame or substrate metal sheet. Another method uses pre-fabricated hot-bent glass-based reflectors, or prefabricated laminated glass-based reflectors, already providing the desired shape, similar to parabolic trough facets. Furthermore, a thin mirror (glass, foil or aluminum) can be attached to a pre-formed sub-structure. Especially during the development of a production process, it is of interest to identify characteristic form errors. This article gives an overview on characteristic surface shape and slope errors of LFC panels. The first part shows experimental results, obtained by deflectometry. The second part introduces a parametric model for the assessment of symmetric surface deviations. Finally, we show the impact of characteristic errors on the focal line, both theoretically and for some typical measured reflectors.

## EXPERIMENTAL - LINEAR FRESNEL COLLECTOR MIRROR PANELS

The geometry of the reflector defines the local surface slopes and local surface normal vectors decisive for the focusing properties of the panels. Therefore, the surface slopes are measured spatially resolved across the panels in order to assess the quality of the reflector shape, which in turn is usually quantified by comparison with an ideal shape, based on deviation maps or slope errors. In this section, we show examples for slope deviation maps and the histograms of

*SolarPACES 2018*
AIP Conf. Proc. 2126, 100003-1–100003-8; https://doi.org/10.1063/1.5117612
Published by AIP Publishing. 978-0-7354-1866-0/$30.00

local surface slope errors of four LFC reflector panels of different production types. We chose examples with different characteristics.

## Measurement Method and Set-up – Fringe Reflection Technique

The local surface slope deviations of the presented linear Fresnel reflector panels were measured with the Fringe Reflection Technique (FRT) at Fraunhofer ISE laboratory, as shown in Figure 1.b. FRT is a deflectometry-based measurement method, originally developed for assessment of small specular objects[1]. FRT was adapted by Heimsath[2, 3] to the assessment of large solar mirrors. Similar techniques were later developed by Andraka[4] and Ulmer[5]. In principle, a camera directed at the mirror surface records a distorted reflection of a sinusoidal pattern. A software algorithm evaluates the pattern and calculates the surface normal for each point imaged in a camera pixel, see Figure 1.a. The advantage of the method is a spatially resolved measurement of the entire reflector area seen by the camera with a fine lateral resolution and information on the shape, surface gradients and microstructure

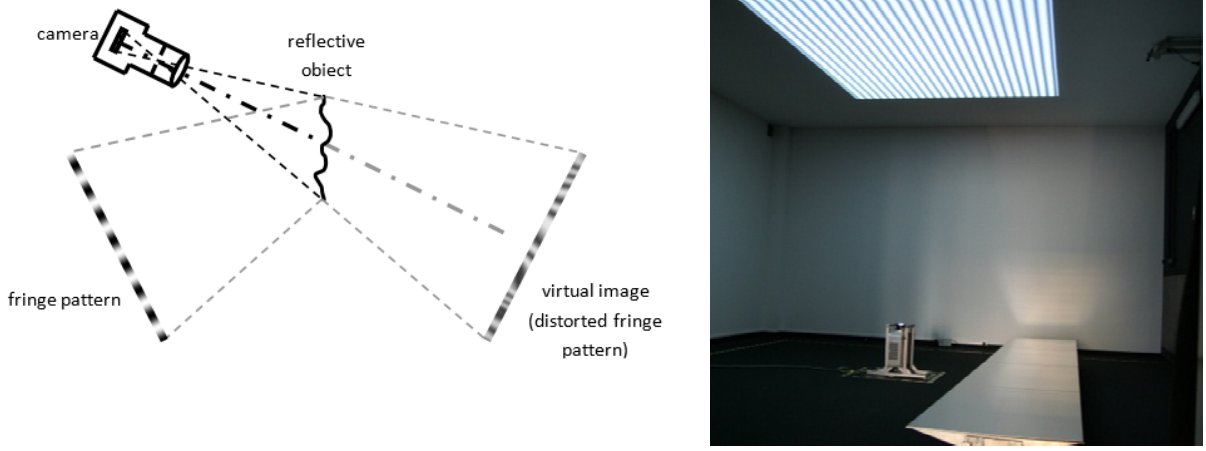


(a) (b)

**FIGURE 1.** (a) A camera records multiple reflected patterns according to a phase-shifting technique. Shape irregularities on the specular surface result in distorted fringe patterns, which are evaluated to determine the actual surface slope. (b) Laboratory set up. The sinusoidal pattern is projected onto a flat, diffuse surface above the sample. A camera (upper right) records the pattern, distorted by local surface errors on the Fresnel reflector panel.

State of the art evaluation of solar mirrors uses the standard deviation or RMS value for characterization of the mirror quality and was first presented by Lüpfert[6]. For line focusing collectors, the local slope deviations are calculated in two directions. The curved, transversal direction is the more relevant one for concentrator analysis. By definition, the curved cross-section lies in the x-z plane. The local slope deviation *sd* is defined as the difference between the measured local surface slope and the slope of the designed, ideal surface. It is evaluated in the curved direction ($sd_x$) and in the flat, longitudinal direction ($sd_y$). The root mean square (RMS) slope deviation in x direction for a reflector with a collector aperture area $A$ is thus

$$SD_{x,rms} = \sqrt{\frac{1}{A}\int\int_A sd_x^2 dxdy} \tag{1}$$

and the standard deviation $\sigma_{sdx}$ of the measured local slope deviations from its mean value $Mean_{sd,x}$ is given by (analogue for $y$ direction)

$$\sigma_{sdx} = \sqrt{\frac{1}{A}\int\int_A (sd_x - Mean_{sd,x})^2 dxdy} \tag{2}$$

## Measured Results for Linear Fresnel Collector Mirrors

This section shows exemplary results for reflector panels with different surface features. Note that the aim is not to characterize one specific mirror and show its quality, but to characterize general features.

Figure 2 shows two reflector panels for small linear Fresnel collectors. In Figure 2.a we see a very first prototype panel before optimization with pronounced systematic errors. The lower panel depicts slope deviations in longitudinal direction of ± 10mrad. The upper picture shows the local slope deviations in the curved direction. Especially the edges deviate from the ideal shape and a waviness is visible. In Figure 2.b we see a different, already optimized panel, with higher shape accuracy.

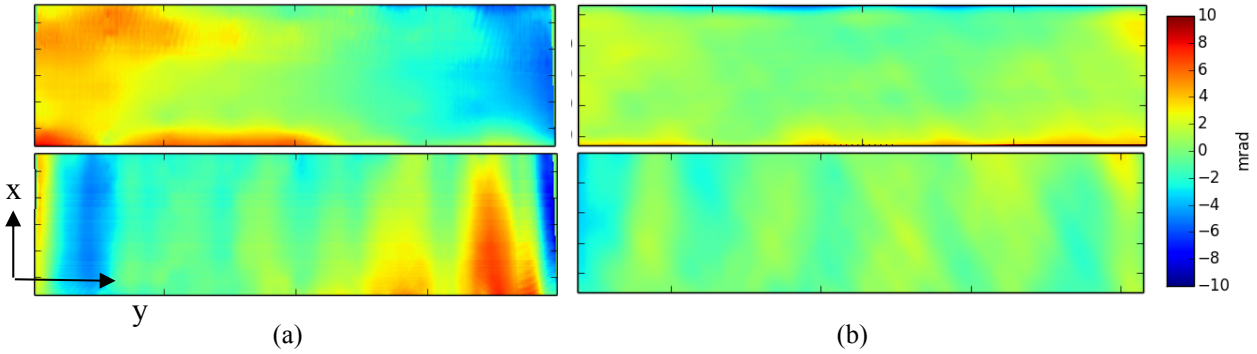


**FIGURE 2.** (a) Local slope deviation map of a LFC reflector panel with large deviations. (b) LFC reflector panel with low slope deviations and good optical quality. Upper picture: Slope deviations in curved x-direction. Lower pictures: Slope deviations in longitudinal y-direction.

In large LFC, the reflector panels often consists of various reflector tiles arranged in longitudinal direction to achieve very long panels. In Figure3, we see again the slope deviation of a first prototype with large slope deviations. Here, each tile and the overall mirror shows specific deformations.

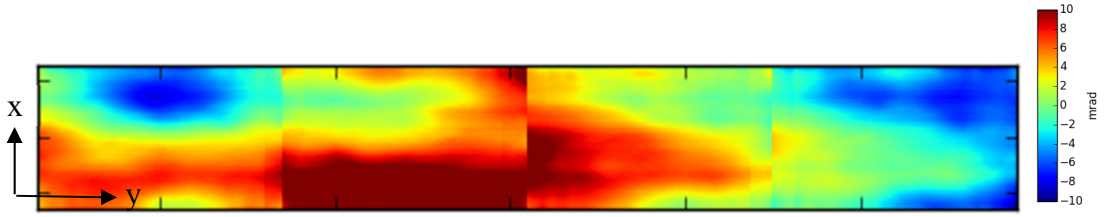


**FIGURE 3.** (a) Local slope deviation map of a LFC reflector panel with large deviations. The panel consists of four mirror tiles.

As example of the statistical evaluation, Figure4 shows the histograms of local slope errors for four different reflector panels. These are compared to the corresponding Gaussian distribution. We see in Figure 4.a that the standard deviation can overestimate the error due to spike values, even though the majority of the errors are very small. Fig, 4.b shows a comparatively broad distribution of surface slope errors. Figure 4.c and 4.d show two pronounced peaks. The standard deviation or RMS value is a very useful number for quality characterization. However, the specific and systematic errors cannot be deduced from it. In addition, the effect of the deviations on the focal line and optical yield may not be represented by it. This is why the following section focuses on the assessment of systematic surface deviations.

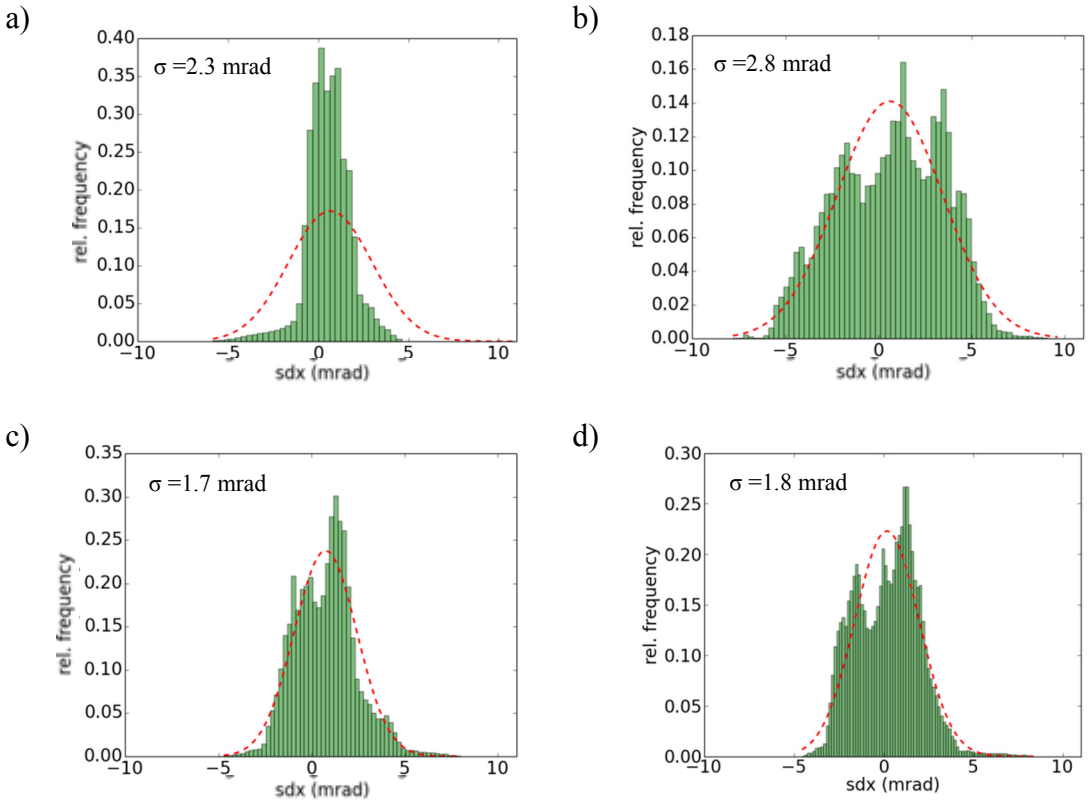


**FIGURE 4.** Histogram of local slope deviations (green bars) and Gaussian distribution corresponding to the calculated standard deviation (red dotted line).

## ASSESSMENT OF SYSTEMATIC SURFACE DEVIATIONS

### Classification of Surface Features

Due to its dimensions (long panels with small width), the LFC reflector panel is prone to specific systematic deviations. The practiced eye can identify these already by looking at the deformation of an ideal sinusoidal pattern on the mirror. To visualize effects in curved and longitudinal direction at once, Figure 5 shows the reflection of a two-dimensional static fringe pattern with a frequency switch, as published in Heimsath2013[3]. In longitudinal direction, the pattern is compressed and widened, which indicates waviness. In curved direction, we see distortions at the edge, hinting at a flattening of the parabola. Further, the diagonal shift of the pattern indicates twist.

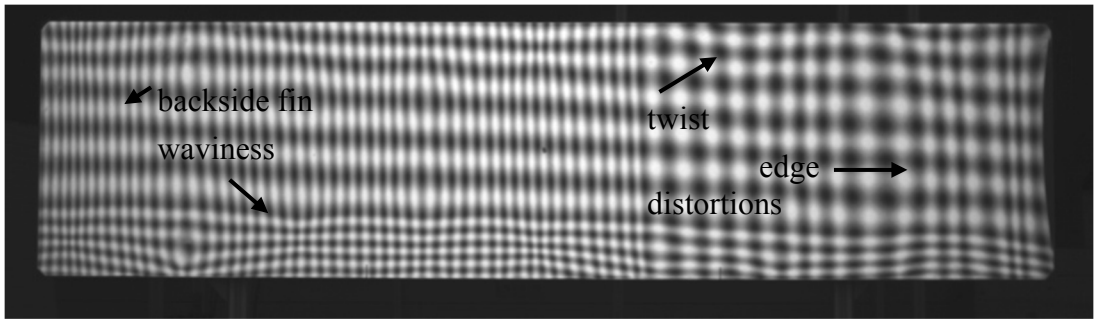


**FIGURE 5.** Reflected static sinusoidal pattern distorted by the non-perfect shape. The original sinusoidal pattern is divided in 4 quadrants of different frequencies in x and y directions, (Heimsath 2013[3]).

We observed typical main features from our laboratory measurements. In curved direction this was typically a bending in the center and relaxation at the edge. This leads to a deviation from the nominal focal length and a widening of the focal line. Undulation in longitudinal direction leads to a longitudinal variation and spots of higher concentration. Furthermore, a rotation of the total reflector or a twist over the length of the reflector leads to a relocation of the focal line. The diagram in Figure 6 shows a scheme for the discussed surface errors, typical for solar concentrators.

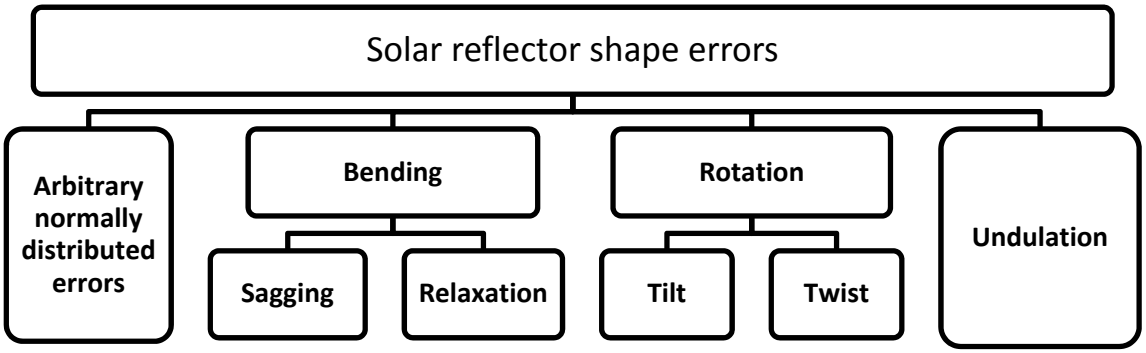


**FIGURE 6.** Categories for solar reflector primary shape errors.

## Parametric Model and Application to Measured Data

The following parametric model includes the observed and classified features. Objective of the model is to identify and quantify systematic surface features. The approach assumes that the total surface can be represented by a convolution of surface functions. It is given by additive combination of the separate geometrical features introduced above, i.e. of a simplified rotation of the parabola (quantified by parameter $a_0$), a parabola with a different focal length and thus additional bending (here described by the parameter $a_1$) and flattening at the edge (parameter $a_3$) and a twist (parameter $a_2$). In longitudinal direction the model includes a tilt of the reflector panel (qantified by parameter $a_4$), twist ($a_5$) sagging in longitudinal direction ($a_6$) as well as twist and undulation (represented by a sinusoidal function with the parameters $a_7$ and $a_8$).

For evaluation the model is applied to all measured data points, this is indicated by the idex i.. First a least square fit routine is applied, the model parameters are found by minimizing the residual between measured and modelled data. Secondly the local slope deviations($sd_{x,i}$ and $sd_{y,i}$ are found by comparing the modelled surface for each data point, here indicated by the index mod, with the ideal durface for each data point, here indicated by the index id.

$$sd_{x,i} = \frac{\partial z_i}{\partial x}_{\mathrm{mod},i} - \frac{\partial z_i}{\partial x}_{id,i} \quad \text{with} \quad \frac{\partial z_i}{\partial x_{\mathrm{mod},i}} = a_0 + a_1 x_i + a_2 y_i + a_3 x_i^3 \tag{3}$$

$$sd_{y,i} = \frac{\partial z_i}{\partial y}_{\mathrm{mod},i} - \frac{\partial z_i}{\partial y}_{id,i} \quad \text{with} \quad \frac{\partial z}{\partial y_{\mathrm{mod},i}} = a_4 + a_5 x_i + a_6 y_i + a_7 \sin\left(a_8 y_i\right) \tag{4}$$

As an example, the following table shows the identified model parameters in curved direction, in accordance with the surface slope deviation data presented in Figure 4.

**TABLE 1.** Coefficients of model function for systematic evaluation of slope errors. Results for selected samples. The coefficients were found by least-square fitting between modelled and measured data.

| **Mirror** | | **$a_{0\ rot}$ (mrad)** | **$1/a_1 = fx_{,bend}$ (m)** | **$a_{2\ twist}$ (rad/m)** | **$a_{3\ bend}$ ($1/m^3$)** |
|---|---|---|---|---|---|
| Sample | 1 | 0.6 | 7.9 | -0.045 | -2.2E-07 |
| Sample | 2 | 0.6 | 5.1 | 5.5E-5 | -2.62E-07 |
| Sample | 3 | 0.7 | 4.3 | 0.001 | 1.92E-09 |
| Sample | 4 | 0.2 | 7.9 | -0.0002 | -1.63E-07 |

## Assessment of the Effect on the Focal Line by Ray Tracing

The simulation of measured local slope deviations is a feature of the Fraunhofer ISE MonteCarlo ray tracing tool chain Raytrace3D[8]. We implemented a feature allowing fast and precise simulation of solar mirrors, the high resolution slope deviation matrices are mapped onto the ideal mirror, interpolation methods are used additionally. Each ray impinging the surface is deflected according to the given slope deviation. This allows us to visualize and compare the effect of the measured and modelled errors. We show the intensity maps in the focal plane of the ideal reflector. A reflector sample with large slope deviations was chosen as an example. The local slope deviations are shown in Figure2.a. In a first step, we simulated the intensity map in the focal plane of an ideal parabola for a virtual sun with a circumsolar ratio of 5%[9] , see Figure 7.(i)a), upper left. Figure 7.(i)b) below shows the focal line that corresponds to a standard deviation of 2.8 mrad, equivalent to the value calculated from local slope deviations, compare also to the histogram displayed in Figure 4.b.

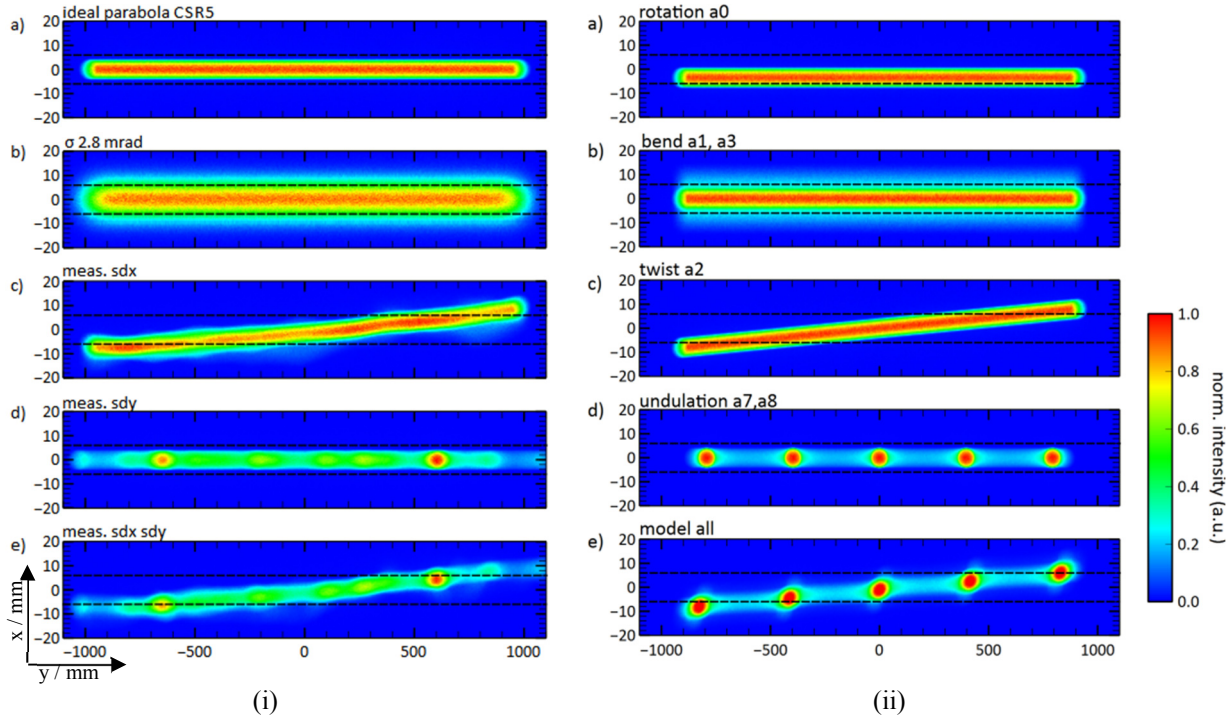


**FIGURE 7.** (i), Left column: a) Ideal focal line with CSR5. b) Focal line with slope error of σ=2.8 mrad. c) Focal line from measured slope deviations in curved direction, d) longitudinal direction e) full measured surface. (ii), Right column: Focal line of a surface according to the model function a) rotation (not by identified value, but by 2 mrad to clearly show the effect), b) bending c) torsion/twist. In longitudinal direction, the effect of undulation d) according to the sinusoidal model function is depicted. e) Modelled combination of all effects. Dotted black lines indicate the designated receiver aperture.

In contrast, the focal lines resulting from the measured slope deviations are shown below, first separately Figure 7.(i)c) $sd_x$ and Figure 7.(i)d) $sd_y$ values and finally for the combined measured errors in Figure 7.e, left. The pictures in the right column Figure 7.(ii)a)-e) show the features as described by the model, using the model parameters $a_0$-$a_3$, $a_7$ and $a_8$ derived from a least-square fit of the model function to the measured data.

The rotation in curved x-direction (represented by coefficient $a_0$) leads to a shift of the focal line in the receiver plane. The rotation results in a noticeable offset of the focal line from the ideal position. Note that the focal line of a rotated panel shown in Figure7.(ii)a) does not show the rotation by a value as shown in Table 1. Instead, a 2 mrad rotation was used to more clearly show the effect of rotation on the focal line. All other parameters result from fitting the model to the measured data. The effect of sagging at the center (coefficient $a_1$) leads to a difference in focal length and in this case to a small widening of the focal line. Flattening at the edges of the glass reflector (caused by material relaxation, coefficient $a_3$) leads to further beam deviations of the reflected radiation resulting in further widening. Twisting of the parabola (coefficient $a_2$) causes a rotation of the gradient field. In consequence, parts of the focal line leave the targeted receiver aperture, as shown in Figure7.(ii)c). Therefore, a twist of the reflector surface might lead to a drastic decrease of the optical efficiency.

In longitudinal direction, large-scale undulation was detected due to fixation of the panel on a specific back structure. This leads to a variation of concentration in longitudinal direction and spots of higher concentration, which might result in high local temperature gradients on the absorber ("hot spots"). They influence the heat transfer to the fluid, cause variations in the . expansion of the steel tube and might impact the stability of the absorber coating if temperatures above the specified limits are reached locally. In contrast, the impact on optical efficiency loss by spillage is small. In analogy, other loss effects in longitudinal direction, such as sagging, have a minor impact on the efficiency but can lead to high local concentration. The simulation results of the modeled surface directly illustrated the impact of the classified slope errors on the focal image and the expected performance loss for line focusing collectors. However, the focal line of the modelled reflector surface displayed in Fig 7.(ii)e) does not exactly describe the modelled line of the measured surface shown in Fig 7.(i)e). One reason for this is that the terms of the parametric model function satisfy particular symmetry relations. They represent either rotational symmetry with respect to the origin (odd terms), rotational symmetric with respect to the y- axis (even terms) or periodic features (sine function with one amplitude and frequency as model parameter). The model does not reproduce non-symmetric features correctly. However, the effect of the classified surface distortions are detected and clearly visualized by the model function. The results emphasize the usefulness of the proposed model for the analysis of systematic surface deformation of the reflector panel. Additionally, the classification and model allows a reciprocal application. By assessing the focal line (ie. By visual inspection or camera-based) we can deduce the shape error and/or installation error causing the distorted focal line. .

## CONCLUSION

In summary, this article discussed typical systematic shape errors of LFC reflector panels. Local slope deviations were shown and compared to the corresponding standard deviations. After identifying tilt, torsion, sagging and bending as main error sources, a parametric model function was introduced. By means of an example case, which exhibits the aforementioned main error sources, the applicability of the model function is demonstrated. Finally, the effect on the focal line was visualized by ray tracing.

The presented method allows a fast detection of systematic surface deformations and improvement of mechanical design and production. By comparing the identified model parameters with reference values, the quantitative contribution of the different main error sources can be readily assessed and compared. The results emphasize the importance of the additional key performance figures bending, rotation and undulation during the development phase of new reflector panels. The presented methodology and derived results advanced the understanding of systematic errors occurring in linear Fresnel collectors and plants.

## ACKNOWLEDGMENTS

The work presented in this article was partly funded by a PhD grant of the Heinrich Böll foundation and Fraunhofer Talenta program.

## REFERENCES


1. T. Bothe et al., “Fringe Reflection for high resolution topometry and surface description on variable lateral scales,” in *Fringe 2005*, edited by W. Osten (Springer, Berlin, Heidelberg, 2006), pp. 362–371.
2. A. Heimsath et al. “Characterization of optical components for linear Fresnel collectors by fringe reflection method,” in Proc. SolarPACES (2008).
3. J. Burke, et al. “Qualifying parabolic mirrors with deflectometry,” J. Eur. Opt. Soc. Rap. Public. 8 (1301) (2013).
4. C. E. Andraka, S. Sadlon, B. Myer, K. Trapeznikov, and C. Liebner, “Rapid reflective facet characterization using fringe reflection techniques,” in (ASME, 2009), Vol. 90163.
5. S. Ulmer et- al, “Automated high resolution measurement of heliostat slope errors,” in Proceedings of SolarPaces (2009).
6. E. Lüpfert and S. Ulmer, "Solar trough mirror shape specifications," Proceedings of solar PACES; 2009, pp. 1-6, 2009.
7. A. Heimsath, G. Bern and P. Nitz, Shape accuracy of solar mirrors - Comparison of two methods using fringe reflection technique, in Proc. SolarPACES (2011)
8. R. Branke and A. Heimsath, “Raytrace3D power tower - A novel optical model for central receiver systems,” in Proc. SolarPACES (2010)
9. D. Buie, A. G. Monger, and C. J. Dey, “Sunshape distributions for terrestrial solar simulations,” (English), Sol Energy, vol. 74, no. 2, pp. 113–122, 2003.